Precise determination of atomic g-factor ratios from a dual isotope magneto-optical trap

I. Chan, B. Barrett, and A. Kumarakrishnan
Department of Physics and Astronomy, York University 4700 Keele Street, Toronto, Ontario M3J 1P3
(Received 31 May 2011; published 19 September 2011)

We demonstrate a technique, for carrying out precise measurements of atomic g-factor ratios, which relies on measurements of Larmor oscillations from coherences between magnetic sublevels in the ground states of ^{85}Rb and ^{87}Rb atoms confined in a dual isotope magneto-optical trap. We show that a measurement of $g_F^{(87)}/g_F^{(85)}$ with a resolution of 0.69 parts per 10^6 is possible by recording the ratio of Larmor frequencies in the presence of a constant magnetic field. This represents the most precise single measurement of $g_F^{(87)}/g_F^{(85)}$ without correcting for systematic effects.

DOI: 10.1103/PhysRevA.84.032509 PACS number(s): 32.10.Dk, 37.10.De, 42.50.Gy, 42.62.Fi

I. INTRODUCTION

Laser cooling and trapping techniques have made it possible to routinely cool neutral atoms to micro-Kelvin temperatures using magneto-optical traps (MOTs). Under these conditions, a significant improvement in a variety of precision measurements has become possible. These include measurements of the natural linewidth [1], atomic structure [2], fountain-based experiments for inertial sensing [3,4] and improvements in atomic clocks [5]. In this paper, we demonstrate a technique, for measuring atomic g-factor ratios, which relies on measurements of Larmor frequencies from ground-state coherences in ^{85}Rb and ^{87}Rb atoms confined in a dual isotope MOT [6]. We show that the ratio of effective atomic g factors can be measured with a resolution of 0.69 parts per 10^6 (ppm), which represents an appreciable increase in single-measurement precision compared to previous papers [7,8]. The experiment exploits the compact dimensions of the sample over which an applied magnetic field can be made highly uniform, and the long observation times that can be obtained using cold atoms. Additionally, the magnetic field is actively stabilized, and magnetizable materials are avoided by utilizing a glass vacuum chamber. The coherent-transient technique exploited in this paper has been utilized previously in room-temperature vapor to study the transfer of coherences between magnetic sublevels [9] and in studies of Zeeman spin echoes [10,11] using far-detuned laser fields.

II. MOTIVATION

Tests of magnetic interactions including g-factor ratios and Zeeman shifts have been carried out previously with a precision of a few ppm in pioneering experiments described in Refs. [7] and [8] using radio-frequency (rf) spectroscopy in near-room-temperature atomic vapors.

The (nonrelativistic) Hamiltonian for an atom in an external magnetic field is

$$H = H_0 + g_J \mu_B \vec{\mathbf{J}} \cdot \vec{\mathbf{B}} + g_I \frac{m_e}{m_p} \mu_B \vec{\mathbf{I}} \cdot \vec{\mathbf{B}}, \tag{1}$$

where H_0 includes the Coulomb and hyperfine interactions and $\vec{\mathbf{B}}$ is the external magnetic field. The constants g_J and g_I are the electron spin orbit g factor and the nuclear g factor, respectively, where g_J is given by

$$g_J = g_L \frac{J(J+1) + L(L+1) - S(S+1)}{2J(J+1)} + g_S \frac{J(J+1) - L(L+1) + S(S+1)}{2J(J+1)}. \tag{2}$$

Here, g_L is the electron orbital g factor, and g_S is the electron g factor. The constants g_S and g_I (in addition to μ_B and m_e/m_p) characterize the Hamiltonian for magnetic interactions. Since g_S [12], m_e/m_p [13], and μ_B [14] are among the most precisely measured quantities in atomic physics, a determination of g_I can be used as an accurate test of atomic theory.

A measurement of g-factor ratios precise to 500 parts per 10^9 (ppb) or better can be used to test corrections to the Hamiltonian for magnetic interactions due to the self-energy of the electron and vacuum polarization. These effects are incorporated into the quantities g_J and g_I as described in Ref. [15]. The corrections to g_J and g_I given in Ref. [15] depend on the nuclear mass and spin (which differ among isotopes) so that measurements of atomic g-factor ratios between different isotopes constitute a sensitive test of specific aspects of quantum electrodynamics. Although the measurement in this paper does not have sufficient precision to test these effects, we demonstrate a proof-of-principle measurement and discuss how our technique can be extended to test predictions discussed in Ref. [15].

For atoms with one outer-shell electron (such as Rb) exposed to small magnetic fields, the relative shift in frequency between atomic sublevels with magnetic quantum numbers differing by 1 ($\Delta m_F = \pm 1$) is quantified in terms of the Larmor frequency ω_L given by

$$\omega_L = g_F \mu_B B/\hbar, \tag{3}$$

where

$$g_F = g_J \frac{F(F+1) + J(J+1) - I(I+1)}{2F(F+1)} - g_I \frac{F(F+1) + I(I+1) - J(J+1)}{2F(F+1)}. \tag{4}$$

It is evident from Eq. (3) that a measurement of ω_L constitutes a measurement of g_F if B can accurately be determined. However, a precise measurement of B at the location of the atoms can be challenging. To avoid this limitation, this

paper measures the Larmor frequencies from ^{85}Rb and ^{87}Rb isotopes (defined as $\omega_L^{(85)}$ and $\omega_L^{(87)}$, respectively) for the same magnetic field so that the ratio of effective atomic g_F factors $g_F^{(87)}/g_F^{(85)} = \omega_L^{(87)}/\omega_L^{(85)}$ can be determined.

The most precise determination of g-factor ratios [7] relied on lamp-based optical pumping to a specific magnetic sublevel in a vapor cell followed by rf excitation to a neighboring sublevel. A magnetic field of $\sim$50 G was used to resolve frequencies of transitions between adjacent ground-state magnetic sublevels to a few tens of hertz using an alternating sequence of measurements in ^{85}Rb and ^{87}Rb. This procedure allowed the ratios $g_I^{(87)}/g_I^{(85)}$ and $g_I^{(85),(87)}/g_J^{(85),(87)}$ to be determined to a few ppm. Since the effect of atom-wall collisions was reduced by paraffin-wall coatings, the linewidth of magnetic dipole transitions was limited only by the homogeneity of the external magnetic field. In this paper, we simultaneously record Larmor oscillations from a weighted sum of $|\Delta m_F| = 1$ coherences from a cold sample of ^{85}Rb and ^{87}Rb isotopes to measure $g_F^{(87)}/g_F^{(85)}$. Although Ref. [15] calculates corrections to g_I and g_J, measurements of $g_F^{(87)}/g_F^{(85)}$ could still be used to test these predictions through Eq. (4).

III. OUTLINE OF EXPERIMENT

The experiment relies on optical excitation of ground-state coherences associated with the $F = 3$ ($F = 2$) hyperfine ground states in ^{85}Rb (^{87}Rb). The geometry of the experiment is shown in Fig. 1(a). An excitation pulse consisting of circularly polarized laser light is incident on a sample of laser-cooled atoms exposed to a weak magnetic field applied orthogonal to the wave vector of the excitation pulse. Figure 1(b) shows allowed optical transitions (solid arrows) that produce coherences between adjacent sublevels of the ground-state manifold. The coherences can be modeled as a magnetization in the sample [16] that precesses in the magnetic field at the Larmor frequency given by Eq. (3). The precession of ground-state coherences can be measured by their effect on a linearly polarized probe pulse with an intensity much less than the saturation intensity. The polarization of the probe pulse is orthogonal to the direction of the magnetic field. The interaction with ground-state coherences produces a rotation in the polarization of the probe pulse due to differential absorption of the σ^+ and σ^- components. The rotation is measured by using a balanced detector consisting of a PBS and two oppositely biased photodiodes as shown in Fig. 1(a) and as described in Ref. [16]. In this scheme, the signal exhibits oscillations at the Larmor frequency. The $\lambda/2$ plate is adjusted so that the sum of the amplified photocurrents is zero when the excitation pulse is turned off and the probe is turned on. The time scale on which Larmor oscillations can be measured should be limited only by the transit time for which atoms remain in the laser beam. For cold-atom experiments, the transit time can be on the order of $\sim$100 ms for the conditions of this experiment (sample temperature $\sim$30 μK, beam diameter $\sim$1 cm). However, we find that cloud launch due to the applied magnetic field limits the maximum time at which Larmor oscillations are resolvable to $\sim$30 ms. Since the required magnetic-field stability further limits the time scale, we only record the first 10-ms window of the signal.

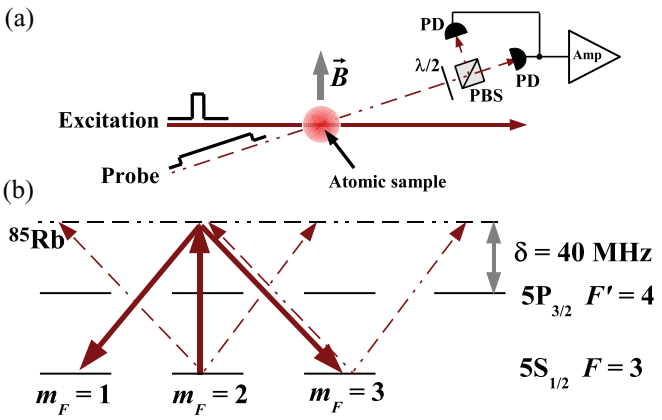

FIG. 1. (Color online) (a) A circularly polarized excitation laser pulse (solid red line) is used to create ground-state coherences. The precession of the resulting coherences in a magnetic field ($\vec{\mathbf{B}}$) is probed with a weak laser pulse (dashed red line) linearly polarized orthogonal to $\vec{\mathbf{B}}$. The angle between the excitation and the probe beams is $\sim$10 mrad in the experiment. Polarizing beam splitter (PBS) and amplifier (Amp). The photodiodes (PD) are oppositely biased. (b) Partial energy-level diagram for ^{85}Rb. Solid red lines show optical transitions excited by the excitation pulse. Since $\vec{\mathbf{B}}$ is orthogonal to the circular polarization of the excitation pulse, $\Delta m_F = \pm 1, 0$ transitions are possible. Dashed red lines show optical transitions excited by the probe pulse. The detuning from atomic resonance is denoted as δ. $|\Delta m_F| = 1$ coherences are possible across the entire ground-state manifold.

IV. EXPERIMENTAL DETAILS

The scheme for trapping ^{85}Rb and ^{87}Rb relies on four independent frequency-stabilized lasers and is illustrated in Fig. 2(a). The light for trapping ^{87}Rb is derived from a Ti:sapphire laser tuned to $\sim$12 MHz below the $F = 2 \rightarrow F' = 3$ transition. The trapping beam for ^{85}Rb is derived from an external cavity diode laser (ECDL) tuned to $\sim$14 MHz below the $F = 3 \rightarrow F' = 4$ transition. The light required to optically pump each isotope into a single-hyperfine state is obtained from two independent repump ECDLs tuned to the $F = 2 \rightarrow F' = 3$ and $F = 1 \rightarrow F' = 2$ transitions in ^{85}Rb and ^{87}Rb, respectively. A single TA is used to amplify the trapping beam for ^{85}Rb and the repump beam for ^{87}Rb as shown in Fig. 2(a). To ensure that the spatial locations of the ^{85}Rb and ^{87}Rb MOTs overlap strongly, the trapping and repump beams for both isotopes are coupled into a single optical fiber. The MOT beams from the fiber are split into six independent paths that intersect along three orthogonal directions in a glass cell as shown in Fig. 2(b). Each beam is expanded to $\sim$6 cm in diameter to provide a large capture volume, allowing up to $\sim 10^9$ atoms to be loaded in the dual isotope MOT. The atom number for each MOT can be optimized independently.

The experimental setup for excitation pulses is shown in Fig. 2(c). To ensure the spatial overlap of the excitation beams, we use a single homebuilt TA to amplify the excitation pulses for both isotopes. The seed beam for ^{87}Rb is derived from a

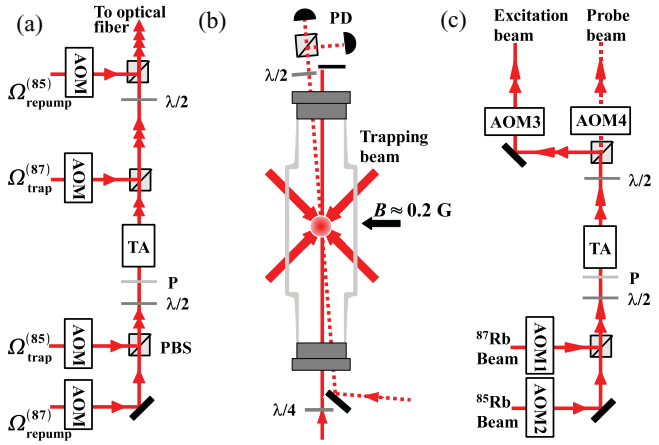

FIG. 2. (Color online) (a) Scheme for trapping two isotopes of Rb. Acousto-optic modulator (AOM), PBS, polarizer (P), tapered amplifier (TA). $\Omega^{(87),(85)}_{\text{trap}}$ and $\Omega^{(87),(85)}_{\text{repump}}$ are the trapping and repump beams, respectively. (b) Orientation of the trapping, excitation, and probe beams. Two pairs of trapping beams are oriented along the diagonal lines, and the third pair is oriented in and out of the page. The excitation (solid red line) and probe (dashed red line) beams are oriented along the vertical lines. (c) Schematic for deriving the excitation beams. AOMs 1 and 2 are used to vary δ for the ^{87}Rb and ^{85}Rb excitation and probe beams. The excitation and probe beams are coupled into separate optical fibers.

frequency-stabilized Ti:sapphire laser, while the ^{85}Rb seed beam is derived from a frequency-stabilized ECDL. Both beams are sent through separate dual-pass AOMs [1 and 2 in Fig. 2(c)] that control the detuning of the excitation and probe beams. The light from these AOMs is combined on a PBS cube and is amplified by the TA. The TA output is divided into two orthogonally polarized beams that serve as the excitation and probe beams. The excitation beam is derived from AOM3, which is pulsed on for 5 μs with a rise time of $\sim$20 ns. Light from AOM4 is used to probe the coherence created by the excitation pulse. The optical power in the probe beam is controlled by varying the rf power-driving AOM4. Both excitation and probe beams are coupled into separate optical fibers. The outputs of these fibers are directed along the vertical axis at a relative angle of 10 mrad through the dual isotope MOT as shown in Fig. 2(b). The power in the excitation and probe beams is $\sim$40 mW and $\sim$2 μW, respectively. The $1/e^2$ radius of both beams is $\sim$0.5 cm. After interacting with the atoms, the probe beam is incident on the balanced detector. The bandwidth of the signal is limited to 2.5 MHz using a low-pass filter.

The apparatus is surrounded by three pairs of square Helmholtz coils of length $\sim$66 cm. Magnetic-gradient canceling coils are wound on the same frames. By using a glass cell and eliminating magnetizable components, it was possible to cancel gradients to the level of 2 mG/cm using these coils and to achieve transit-time-limited experiments. The magnetic field produced by these coils is monitored using a three-axis flux-gate magnetic sensor placed just outside the glass chamber. One pair of Helmholtz coils provides the uniform static magnetic field of $\sim$0.2 G required to produce Larmor oscillations in the signal [**B** in Fig. 2(b)]. The other two pairs of Helmholtz coils ensure that background fields are canceled to the level of $\sim$100 μG along the other two orthogonal directions as measured by the flux-gate sensors. The three-axis sensor is used to provide a feedback signal to the power supplies used for the magnetic-field control. During the trapping phase, the feedback is disengaged, and the power supplies provide steady currents to all three Helmholtz coils. After the trapping gradient is turned off, the feedback is engaged to suppress time-varying fields along three orthogonal directions that can cause small changes in the Larmor frequency over the duration of the signal.

At the start of the experiment, both ^{85}Rb and ^{87}Rb atoms are loaded simultaneously from the background vapor for $\sim$700 ms into a dual isotope MOT. CCD camera images show that the centers of these traps, which have typical $1/e^2$ radii of $\sim$3 mm, are overlapped to within $\sim$1 mm. We have verified that loading a given isotope does not affect the number of trapped atoms for the other isotope. The magnetic-field gradient for the MOT is turned off in $\sim$500 μs, and both isotopes are cooled in an optical molasses for 60 ms to allow transient effects from turning off the gradient to decay. The trapping beams for both isotopes are then shifted $\sim$70 MHz below resonance for 5 ms to cool the atoms to $\sim$30 μK. The excitation pulses for both isotopes are applied following a dark time of 200 μs. The coherence is probed for $\sim$10 ms, and the resulting signal is digitized on an oscilloscope. The record length for each single-shot measurement that lasts 10 ms consists of 200 000 points with a resolution of 50 ns.

V. RESULTS AND DISCUSSION

For the detection scheme in Fig. 1(a), the expected signal shape is a pure sinusoid for a single isotope. The signal from both isotopes consists of oscillations at the Larmor frequencies $\omega_L^{(85)}$ and $\omega_L^{(87)}$ resulting in a beat note, which is shown in Figs. 3(a) and 3(b). The signal is fit to a function of the form

$$e^{-(t/\tau)^2}\left[a_1\cos\left(\omega_L^{(85)}t+\phi_1\right)+a_2\cos\left(r\omega_L^{(85)}t+\phi_2\right)\right], \qquad (5)$$

where a_1 and a_2 are the signal amplitudes for ^{85}Rb and ^{87}Rb, respectively, τ is the decay constant, and ϕ_1 and ϕ_2 are arbitrary phase factors. We find that using a Gaussian decay term in the fit function gives a slightly narrower distribution of residuals compared to using an exponential decay term. This indicates that the decay due to the transit-time atoms through the laser dominates the exponential decay caused by decoherence due to the probe pulse. We find that the functional form of the decay (Gaussian or exponential) term does not influence the final result. Typical values for τ were $\sim$7 ms. The quantity r in Eq. (5) is the ratio of atomic g_F factors $g_F^{(87)}/g_F^{(85)}$, which can be extracted to a precision of $\sim$1.5 ppm from a single trace. We find that fitting to the first 5 ms of the signal gives us the minimum uncertainty in $g_F^{(87)}/g_F^{(85)}$ due to variations in ω_L associated with ac magnetic fields. The value of $g_F^{(87)}/g_F^{(85)}$ extracted from the fits is consistent with expectations based on Eqs. (3) and (4). Figure 3(c) shows 75 single-shot measurements from signals similar to Fig. 3(a). These measurements were recorded over a time scale of $\sim$3 min over which the magnetic field was stabilized at $\sim$10 μG. The mean value of the distribution shown in Fig. 3(c) is $\bar{r} = 1.498\,8871(10)$ (the digits in parentheses represent the uncertainty in the last two

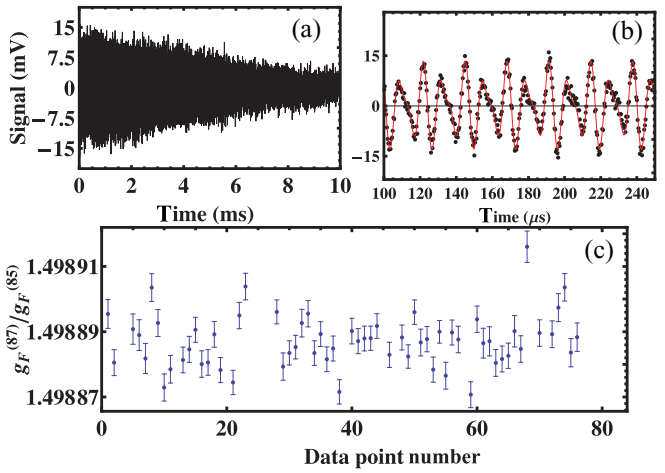

FIG. 3. (Color online) (a) Ground-state coherence signal from the dual isotope MOT. (b) Closeup of the data displayed in (a) showing multiple-frequency components in the signal. Only one eighth of the points are displayed so that the fit (red line) and the data (black dots) can be distinguished. From a single shot, the ratio of effective atomic g factors $r = g_F^{(87)}/g_F^{(85)}$ is typically determined to a precision of ~ 1.5 ppm. (c) Seventy-five data sets taken over ~ 3 min. The error bars represent the fit uncertainties. The mean value is $\bar{r} = 1.498\,8871$, and the (1σ) standard deviation of the mean is 1.0×10^{-6} (0.69 ppm). The reduced χ^2 is 1.1 for this distribution.

digits of $\bar{r}$) and constitutes a single measurement of $g_F^{(87)}/g_F^{(85)}$ precise to 0.69 ppm. This uncertainty represents the standard deviation of the mean. From Fig. 3(c), it is clear that there is scatter in the data that are larger than the fit uncertainties. This is possibly due to fluctuations in the probe power. However, the distribution shown in Fig. 3(c) has a reduced χ^2 of 1.1 and is consistent with a Gaussian distribution having the quoted mean and standard deviations.

Using Eq. (4), we find that there is an ~ 16-ppm discrepancy between the results of Ref. [7] and the value of $g_F^{(87)}/g_F^{(85)}$ extracted from Fig. 3. As discussed in the next section, this discrepancy is smaller than the extent of systematic effects estimated on the basis of numerical simulations and experimental studies.

VI. DISCUSSION OF SYSTEMATIC EFFECTS

Systematic effects in the measured value of $g_F^{(87)}/g_F^{(85)}$ arise due to shifts in the Larmor frequency due to ac Stark shifts and the Breit-Rabi effect [17]. Other effects, such as energy-level shifts due to cold-cold collisions are on the order of millihertz [18] and are not detectable.

The ac Stark-shift systematic is caused by the relative shift in energy between adjacent ground-state sublevels, which depends on the intensity and detuning of the probe pulse [16]. The shift in $g_F^{(87)}/g_F^{(85)}$ is ~ 10 ppm per μW/cm^2 for $\delta = 40$ MHz based on initial surveys. There is no Stark shift due to the excitation pulse, which is turned off before the probe pulse is switched on.

Although we have assumed that $g_F^{(87)}/g_F^{(85)}$ is independent of B based on Eq. (3), the Breit-Rabi effect causes a nonlinear dependence of ω_L on B so that the magnetic-field term in Eq. (3) does not cancel when the ratio of Larmor frequencies is measured. This effect, in turn, causes a systematic shift that depends on the magnitude of the applied field. Additionally, the nonlinear variation in ω_L on B depends on m_F. Therefore, different $|\Delta m_F| = 1$ coherences across the ground-state manifold precess at different Larmor frequencies. Since the signal consists of a weighted sum of coherences from different ground-state sublevels, the measured value of $g_F^{(87)}/g_F^{(85)}$ depends on the distribution of magnetic-sub-level populations in the ground state. Assuming an applied field of 0.2 G and that only coherences from the extreme magnetic sublevels for both isotopes ($m_F = 3 \leftrightarrow m_F = 2$ coherence for ^{85}Rb and $m_F = 2 \leftrightarrow m_F = 1$ coherence for ^{87}Rb) contribute to the signal, the shift in $g_F^{(87)}/g_F^{(85)}$ is estimated to be ~ 90 ppm based on the Breit-Rabi formula. However, if there are contributions to the signal from coherences other than those associated with the extreme state sublevels, the Breit-Rabi shift can be reduced to the order of ~ 10 ppm. We find that the interpretation of this systematic effect is complicated because the relative amplitudes of coherences that contribute to the signal also depend on the magnetic field.

Since the measured value of $g_F^{(87)}/g_F^{(85)}$ depends on B, it could be expected that fluctuations in the applied magnetic field could cause scatter in a distribution of measurements of $g_F^{(87)}/g_F^{(85)}$. As mentioned in the discussion relating to Fig. 3(c), the magnetic-field stability was 10 μG, which ensures that the scatter in the measured distribution of $g_F^{(87)}/g_F^{(85)}$ is negligible (~ 5 ppb).

Since the magnitude of the shift in the measured value of $g_F^{(87)}/g_F^{(85)}$ due to the ac Stark shift and the Breit-Rabi effect depends on how the coherences are distributed among the ground state, we use multilevel numerical simulations based on Ref. [19] to study the distribution of coherences. The numerical simulations rely on solving for the time-evolution of the off-diagonal elements of the atomic density matrix based on differential equations containing terms that model the atom-laser coupling and magnetic interaction. The solutions for ρ_{m_F,m_F+1}, as a function of time, represent ground-state coherences precessing at the Larmor frequency. The atom-laser coupling is written in the interaction representation, which pertains to a frame of reference rotating at the atomic transition frequency ω_0 ($\omega_0 = \omega_{F=3\rightarrow F'=4}$ for ^{85}Rb and $\omega_0 = \omega_{F=2\rightarrow F'}$ for ^{87}Rb) as described in Ref. [19]. The terms describing the magnetic interaction represent the frequency shifts of the individual magnetic sublevels due to the magnetic field. The model includes the $F = 2,3$ and $F' = 1$–4 levels in ^{85}Rb and the $F = 1,2$ and $F' = 0$–3 levels in ^{87}Rb. To compare simulations with experimental results, we compute a summation of the calculated coherences ($\sum \rho_{m_F,m_F+1}$) for both isotopes and extract the ratio of Larmor frequencies as a function of experimental parameters (magnetic field, probe power, and detuning). We find that the simulations are qualitatively consistent with experimental results and show that the relative amplitudes of coherences contributing to the signal vary with probe-laser parameters and magnetic field.

VII. CONCLUSIONS AND FUTURE WORK

To summarize, we have demonstrated a technique for precisely measuring atomic g-factor ratios from a sample

of laser-cooled ^{85}Rb and ^{87}Rb atoms confined to a dual isotope MOT and exposed to a constant magnetic field. Using this technique, we have obtained a single measurement of $g_F^{(87)}/g_F^{(85)}$ with a statistical uncertainty of 0.69 ppm in $\sim$3 min of data acquisition. The short data-acquisition time required to obtain high-precision measurements suggests that the technique is well suited for studies of systematic effects. We also find that the probe intensity required to study systematic effects due to the ac Stark shift is about ten times lower than in an alternative technique that also exploits magnetic-sub-level coherences [20].

The technique presented in this paper measures a single Larmor frequency from a weighted sum of ground-state coherences. This technique can be extended to test relativistic theories, such as in Ref. [15], by resolving Larmor oscillations from individual coherences in the ground-state manifold. Such a measurement can be accomplished by using a stronger magnetic field ($\sim$5 G) that is rapidly turned on after atoms are released from the MOT. This makes it feasible to measure ratios of spin orbit (g_J) and nuclear (g_I) g factors through the Breit-Rabi formula as in Ref. [7]. However, the experiment would require measurements of Larmor oscillations from coherences in the $F = 2$ ($F = 1$) ground state of ^{85}Rb (^{87}Rb) in addition to measurements of Larmor oscillations from the $F = 3$ ($F = 2$) ground state of ^{85}Rb (^{87}Rb) reported in this paper. Combined with studies of systematic effects, high-precision measurements (better than 500 ppb) of atomic g-factor ratios can be obtained.

ACKNOWLEDGMENTS

This work was supported by the Canada Foundation for Innovation, Ontario Innovation Trust, Natural Sciences and Engineering Research Council of Canada, Ontario Centres of Excellence, and York University. We would like to acknowledge the contributions of Robert Berthiaume and Vlad Popovici in the construction of diode lasers and tapered amplifiers, Scott Beattie for his involvement in the construction of the vacuum system, and Adam Carew and Carson Mok for assisting with data acquisition relevant to systematic effects. We would also like to acknowledge helpful discussions with Eric Hessels of York University.

[1] C. W. Oates, K. R. Vogel, and J. L. Hall, Phys. Rev. Lett. **76**, 2866 (1996).
[2] T. Kisters, K. Zeiske, F. Riehle, and J. Helmcke, Appl. Phys. B **59**, 89 (1994).
[3] M. Kasevich and S. Chu, Phys. Rev. Lett. **67**, 181 (1991).
[4] A. Peters, K. Y. Chung, and S. Chu, Nature (London) **400**, 849 (1999).
[5] G. Santarelli, P. Laurent, P. Lemonde, A. Clairon, A. G. Mann, S. Chang, A. N. Luiten, and C. Salomon, Phys. Rev. Lett. **82**, 4619 (1999).
[6] W. Süptitz, G. Wokurka, F. Strauch, P. Kohns, and W. Ertmer, Opt. Lett. **19**, 1571 (1994).
[7] C. W. White, W. M. Hughes, G. S. Hayne, and H. G. Robinson, Phys. Rev. **174**, 23 (1968).
[8] C. Cohen-Tannoudji and A. Kastler, *Progress in Optics*, Vol. V (Elsevier, Amsterdam, 1966).
[9] D. Suter, H. Klepel, and J. Mlynek, Phys. Rev. Lett. **67**, 2001 (1991).
[10] M. Rosatzin, D. Suter, and J. Mlynek, Phys. Rev. A **42**, 1839 (1990).
[11] D. Suter, M. Rosatzin, and J. Mlynek, Phys. Rev. Lett. **67**, 34 (1991).
[12] D. Hanneke, S. Fogwell, and G. Gabrielse, Phys. Rev. Lett. **100**, 120801 (2008).
[13] D. L. Farnham, R. S. VanDyck, and P. B. Schwinberg, Phys. Rev. Lett. **75**, 3598 (1995).
[14] P. J. Mohr, B. N. Taylor, and D. B. Newell, Rev. Mod. Phys. **80**, 633 (2008).
[15] J. M. Anthony and K. J. Sebastian, Phys. Rev. A **49**, 192 (1994).
[16] D. Suter and J. Mlynek, Phys. Rev. A **43**, 6124 (1991).
[17] A. Corney, *Atomic and Laser Spectroscopy*, Vol. V (Oxford University Press, Clarendon, 1977).
[18] S. J. J. M. F. Kokkelmans, B. J. Verhaar, K. Gibble, and D. J. Heinzen, Phys. Rev. A **56**, R4389 (1997).
[19] P. Berman and V. S. Malinovsky, *Principles of Laser Spectroscopy and Quantum Optics* (Princeton University Press, Princeton, 2011).
[20] I. Chan, A. Andreyuk, S. Beattie, B. Barrett, C. Mok, M. Weel, and A. Kumarakrishnan, Phys. Rev. A **78**, 033418 (2008).